Scientific paper

Minerals From Macedonia. XXI. Vibrational Spectroscopy as Identificational Tool for Some Phyllosilicate Minerals

Violeta Šontevska,[a] Gligor Jovanovski,[a,b,*] Petre Makreski,[a] Aleksandra Raškovska[a] and Bojan Šoptrajanov[a,b]

[a]*Institute of Chemistry, Faculty of Science, Ss Cyril and Methodius University, Arhimedova 5, P.O. Box 162, 1001 Skopje, Republic of Macedonia*

[b]*Macedonian Academy of Sciences and Arts, Bul. Krste Misirkov 2, P.O. Box 428, MK-1001 Skopje, Republic of Macedonia*

** Corresponding author: E-mail: gligor@iunona.pmf.ukim.edu.mk*

Received: 14-01-2008

Dedicated to the memory of Professor Ljubo Golič

Abstract

Vibrational (infrared and Raman) spectra of the sheet silicate minerals: biotite, $K(Mg,Fe^{2+})_3AlSiO_{10}(OH,F)_2$; muscovite, $KAl_2(Si_3Al)O_{10}(OH,F)_2$; phlogopite, $KMg_3(Si_3Al)O_{10}(F,OH)_2$ and sheridanite (clinochlore), $(Mg,Al)_6(Si,Al)_4O_{10}(OH)_8$, collected from various localities within the Republic of Macedonia, were described and interpreted. The above-mentioned minerals showed IR spectral similarities in the region bellow 1200 cm^{-1} mainly due to their common structural characteristics. In general, the bands appearing in the 1100–900 cm^{-1} spectral region were assigned to ν(Si–O–Si) modes, whereas most of the lower-frequency bands were interpreted as either δ(OH) or δ(Si–O–Si) vibrations. The similarities between the Raman spectra (1200-100 cm^{-1}) were less pronounced indicating that Raman technique is more sensitive to compositional changes. The results were compared to the literature data for the analogous species originating from all over the world. The authenticity of the samples was checked by powder XRD and chemical composition determined by X-ray microprobe analysis.

Keywords: Vibrational spectroscopy, mica, identification, phyllosilicates.

1. Introduction

As a continuation of our previous work concerning the spectra-structural study of several sheet silicates[1], the vibrational spectra of additional four sheet silicate minerals (mainly from the mica group) collected from various regions of Republic of Macedonia are studied. Although the samples exhibit marked similarities in their spectra, an attempt was made to correlate the spectral characteristics of the collected minerals with their structural features. For the aim of the investigations, the obtained IR and Raman spectra were interpreted and the results were compared with the literature data for the analogous mineral species from various localities throughout the world.

Several studies have been so far undertaken to describe the vibrational spectra of muscovite[2–11], and phlogopite[4–6,9,11–16]. On the other hand, the IR spectrum of biotite is only presented in mineral Atlas[5] and Internet[6] whereas its Raman spectrum is found in Internet databases[17,18]. In addition, to the best of our knowledge, neither infrared nor Raman data have been found in the literature for sheridanite mineral. Therefore, the results from this work bring clearer insight on the vibrational spectral characteristics of this geologically important mineral group.

2. Experimental

The sheet silicate minerals were collected from various localities[i]: muscovite (Dunje, Nežilovo), biotite (Pelagon, Čanište), phlogopite and sheridanite (Sivec). The crystals of the investigated minerals were mechanically

[i] The geographical position of the various localities can be found in Ref.[19]

separated from the ore and carefully picked up under an optical microscope and used in a powdered form.

The Perkin-Elmer FTIR System 2000 interferometer was employed for recording the spectra using the KBr pellet method and the Nujol suspension mulls.

In order to obtain representative spectra of the samples, the Raman measurements were performed using three excitation lines. The computerized Dilor Z24 triple dispersive monochromator with Coherent Innova 400 argon ion laser operating with the 514.5 nm excitation line was a first choice. Depending on the mineral sensitivity, a laser power of 50 or 100 mW was applied. To reduce the heating of the sample during the recording process, the incident laser beam was modified in line-shape focus. The Raman effect for some of the samples was monitored using 532 nm YAG laser line from micro-Raman multichannel spectrometer – Horiba JobinYvon LabRam Infinity (power of 7 mW and focal length *f* x 100). Some Raman measurements were carried out on Bruker FT model 106/S connected to the FT interferometer Equinox 55 using 1064 nm excitation line of Nd-YAG frequency laser (FT Raman spectra). The resolution in both IR and Raman spectra is 4 cm^{-1}.

The measurements were carried out at a room temperature and GRAMS/32 software package was applied for the spectral manipulations.

Philips Analytical X-ray diffractometer PW 3710 was used for X-ray powder diffraction (step 0.01°, time per step 2.5 s). Generator with 50 kV and current of 30 mA employed as a source for Cu*K*α radiation. The unit cell parameters were calculated from their X-ray diffraction patterns using CRYSFIRE software. The obtained values were refined using CHECKCELL (a modified version of CELREF for analysing the solutions given by the CRYSFIRE).

Chemical composition of the minerals was analyzed by electron microprobe analyzer (EMS) CAMECA. The presented mineral analyses represent the average values obtained from three different points.

3. Crystallographic Data and Powder XRD Analysis

The basic building blocks of all silicate minerals are the tetrahedra consisting of four O atoms arranged to occupy the corners of a tetrahedron with a Si atom in the center. The silicon tetrahedra may polymerize so that, in case of sheet silicates, three oxygens are shared between adjacent tetrahedra to form continuous sheets that are combined in TO and TOT layers (T – tetrahedral, O – octahedral sheet). As a result of possible substitution in the tetrahedral (Al^{3+} is the ion that more frequently substitutes Si^{4+}) and in the octahedral sites (where R^{2+} and R^{3+} ions are substituted by R^{+} and R^{2+} ions, respectively[21]), the net negative charge in the TOT layers is balanced by inserting cations. The bonding between the adjacent TOT layers in muscovite, phlogopite and biotite includes both van der Waals bonds and stronger ionic bonds involving the interlayer cations, whereas in the case of sheridanite the layers are linked by hydrogen bonds[20].

The micas have the general formula $IM_{2-3}\square_{1-0}T_4O_{10}X_2$. The interlayer sites (I) are usually occupied by K^{+}, Na^{+}, Ca^{2+} ions; M (the octahedral cations) are Mg^{2+}, Al^{3+}, Fe^{3+}; T (the tetrahedral cations) are mostly Al^{3+} and Si^{4+}; □ is vacancy in the structure while X (anions) are OH^{-}, F^{-} [21]. The crystallographic parameters for the studied minerals are given in Table 1, whereas the most important crystal features are summarized below:

(1) The muscovite crystallizes in the monoclinic *C*2/*c* crystal structure.[22] The structural sheets contain two tetrahedral sites T1 and T2, where approximately 75% of these sites are randomly occupied by Si^{4+}, while the remaining 25% contain Al^{3+}. The sheets are bonded together by K^{+} layers and dioctahedral layers, where Al^{3+} occupy the M2 octahedral sites (coordinated by four non-bridging O atoms as well as by two OH groups). The M1 octahedral sites are vacant[8]. The sodium analogue of muscovite is paragonite[23] $[NaAl_2(Si_3Al)O_{10}(OH)_2]$.

(2) The atomic arrangement in the phlogopite structure is similar to that in muscovite. Noticeable difference between the two structures is related to the occupation of the octahedral sites M1 and M2. Namely, in the phlogopite structure these sites are filled with Mg^{2+} cations, whereas in the case of the muscovite structure only one octahedral site is occupied by Al^{3+} cations. Each Mg atom in phlogopite is octahedraly coordinated with four O atoms from the tetrahedral sheets and two F and/or OH ions[15].

(3) The biotite group, often referred as trioctahedral dark mica, can be described in terms of four endmembers: phlogopite, annite, eastonite and siderophyllite[24,25]. In the biotite structure, Fe^{2+} substitute octahedral Mg^{2+} cations. Other substitutions include Ca^{2+}, Ba^{2+} and Cs^{+} and especially Na^{+} for K^{+} as well as F^{-} for OH^{-} [20].

(4) The studied mineral designated as sheridanite $[(Mg,Al)_6(Si,Al)_4O_{10}(OH)_8]$ according to the Strunz classification system[26] belongs to mica-like minerals with $[Si_4O_{10}]^{4-}$ group and represents a less known variety of chlinochlore (Mg-rich chlorite). The general formula of chlorite is $X_{4-6}Y_4O_{10}(OH,O)_8$, where X denotes either Al, Fe, Mg, Li or rarely Cr; Y represents either Al, Si, B or Fe, but mostly Al and Si[27].

The powder XRD of the minerals was performed for the identification purposes (Table 1). It should be pointed out that the calculated unit cell parameters *a* and *c* for

muscovite, biotite and phlogopite are oppositely arranged (Table 1) compared to corresponding parameters taken from the literature (*a* axis in the latter mineral being approximately twice larger, as well). The relation between the literature data (a_l, b_l, c_l) and the calculated data (a_c, b_c, c_c) from the powder XRD for sheridanite is as follows: $a_l = b_c$; $b_l = 2c_c$; $c_l = a_c$.

The assignment of the bands below 1150 cm^{-1} in the vibrational spectra of all studied minerals is to some extent tentative because the investigations could not be carried out in details without further experiments (for example, the use of the isotope substitution and dilution technique). However, the bands in the 1150–950 cm^{-1} are attributed to the stretching Si–O–Si or Si–O–Al modes[10] (although Al may replace Si in the tetrahedral sites, normally two consecutive tetrahedra are not, for geometrical considerations, occupied both by Al, and the bonds are Si–O–Si or Al–O–Si) whereas the bands in the 900–740 cm^{-1} arise due to the octahedral Al–O and Al–O–Al stretching modes[11] (Table 2). The shifting of the shoulder (1080–1065 cm^{-1}) positioned on the higher frequency side of the strongest IR band is explained by the compositional change of the mica going from muscovite to celadonite[11] (Table 2). Taking into account this consideration and the appearance of the shoulder at 978 cm^{-1} it could be tentatively assumed that the studied mineral composition is very close to muscovite. In addition, a noticeable wavenumber decrease (from 538–519 cm^{-1}) of the bending O–Si–O vibration occurs as the composition becomes tetrasilicic[11]. The results from the X-ray microprobe analysis are found to be similar to those obtained for the muscovite sample from Dunje (w.t. K_2O – 11.19%; Na_2O <0.01%; MgO – 2.56%; CaO <0.01%; FeO – 4.03%; SiO_2 – 49.18%; TiO_2 – 0.37%; MnO < 0.01%; Al_2O_3 – 28.40%).

Table 1. The crystallographic parameters of the studied sheet silicate minerals

Mineral	Crystal system	Space group	Unit cell parameters (a, b, c in Å, β in °)
Muscovite (Dunje)	Monoclinic	*C*2/*c*	a = 5.1918, b = 9.0153, c = 20.0457, β = 95.74, Z = 4; Ref. 28
			a = 19.9733, b = 9.0601, c = 5.2261, β = 95.81, Z = 4 (this work)
Phlogopite (Sivec)	Monoclinic	*C*2/*m*	a = 5.3080, b = 9.1900, c = 10.1550, β = 100.08, Z = 4; Ref. 29
			a = 20.2614, b = 9.0557, c = 5.3275, β = 100.16, Z = 8 (this work)
Biotite (Pelagon)	Monoclinic	*C*2/*m*	a = 5.3000, b = 9.2100, c = 10.1600, β = 99.50, Z = 2; Ref. 30
			a = 10.2255, b = 9.2558, c = 5.3520, β = 100.21, Z = 2 (this work)
Sheridanite (Sivec)	Monoclinic	*C*2/*m*	a = 5.3200, b = 9.2100, c = 28.4800, β = 97.90, Z = 4; Ref. 31
			a = 28.5397, b = 5.3248, c = 4.7039, β = 97.26, Z = 2 (this work)

4. Results and Discussion

4. 1. Muscovite, $KAl_2(Si_3Al)O_{10}(OH,F)_2$

The powder IR absorption spectra in the region from 4000 to 400 cm^{-1} (Fig. 1, a and b) as well as the Raman spectra in the wavenumber range 1200–110 cm^{-1} (Fig. 2, a–d) of muscovite and the mineral firstly designated as paragonite (according to the morphological features) are studied together in order to demonstrate their resemblance. However, the absence of Na according to the chemical analysis of the sample from Nežilovo (w.t. K_2O – 10.13%; Na_2O <0.01%; MgO – 1.02%; CaO <0.01%; FeO – 4.76%; SiO_2 – 48.12%; TiO_2 – 0.38%; MnO – 0.40%; Al_2O_3 – 23.72%) confirms that the studied sample is muscovite (not paragonite). Furthermore, the results from the X-ray microprobe analysis are found to be similar to those obtained for the muscovite sample from Dunje (w.t. K_2O – 11.19%; Na_2O <0.01%; MgO – 2.56%; CaO <0.01%; FeO – 4.03%; SiO_2 – 49.18%; TiO_2 – 0.37%; MnO < 0.01%; Al_2O_3 – 28.40%).

The IR spectra of the studied samples are practically identical and are characterized by bands that appear in two well-defined spectral regions originating from OH and SiO_4 (including MO_6 modes) vibrations respectively (Fig. 1, a and b). In the OH stretching region, a band with medium intensity is registered around 3610 cm^{-1} and attributed to the stretching vibrations of the OH groups. In addition, a weak and broad band found around 3425 cm^{-1} originate from the H_2O stretching vibrations from the adsorbed water. The presence of the adsorbed water in both samples is also evident from the weak band around 1630 cm^{-1}, ascribed to $\delta(H_2O)$ vibrations. The assignments of the IR bands as well as their comparison with the literature data are given in Table 2.

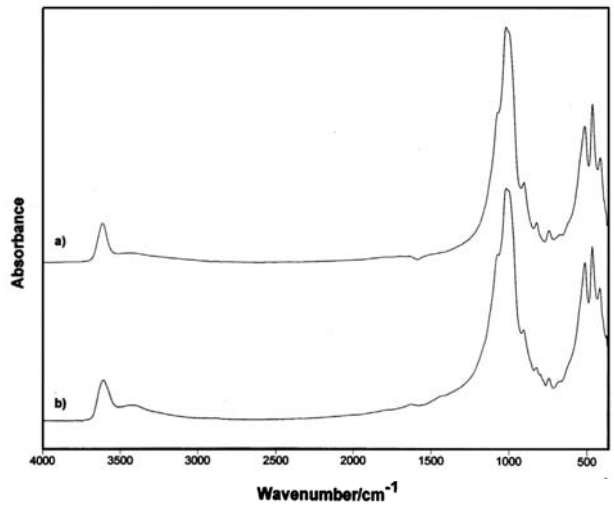

Fig. 1. FT IR spectra of muscovite from Dunje (a) and Nežilovo (b) obtained using KBr pellets.

Table 2. Assignment of the bands in the powder infrared spectrum of muscovite samples

This work (Dunje)	This work (Nežilovo)	Taylor et al.[2]	Veder & McDonald[3]	Stubičan & Roy[4]	Zeller & Juszli[5]	Langer at al.[10]	Tentative assignment
3615 m[a]	3610 m	3640 w	3628 m	3620 m[b, c]	3630 m[b, c]	–	ν(OH)
3430 vw	3422 w	3430 vw	–	–	3420 w	–	$\nu(H_2O)$
1630 vw	1630 w	1630 vw	–	–	1630 w	–	$\delta(H_2O)$
–	–	–	1120 w	–	–	1113	
1078 sh	1076 sh	1065 sh	1070 sh, s	1080 sh	1070 sh	1065	ν_{as}(Si–O)
1025 vs	1022 vs	1020 vs	1024 vs	1020 vs	1020 vs	1028	ν_{as}(Si–O)
1001 sh, s	999 sh, s	–	985 sh, s	–	–	996	ν(Si–O–Si)
–	–	–	–	–	–	937	
910 w	908 w	920 sh	928 m	915 w	920 sh	912	L(Al–O–H)[d]
–	–	–	–	–	–	877	
827 w	825 w	822 w	827 m	820 w	825 w	831	ν(Al–O)
–	801 vw	795 vw	805 w	800 vw	–	805	ν(Al–O–Al)
748 w	746 w	765 w	755 w	760 w	755 m	751	ν(Al–O–Al)
–	–	–	–	–	–	727	
690 vw	692 vw	–	691 w	–	690 w	700	δ(Si–O–Al)
626 sh	624 sh	–	630 w	–	–	619	δ(Si–O–Si)
–	–	–	–	–	–	580	
558 sh	557 sh	–	–	–	–	553	δ(Si–O–Si)
–	–	–	–	–	–	539	
521 s	519 s	538 s	528 s	535 s	535 s	520	δ(Si–O–Si)
472 s	470 s	472 s	472 s	475 s	475 s	480	δ(Si–O–Si)
416 s	415 s	410 m	408 s	405 w	405 s	410	L(Al–O–H)[d]
–	–	–	–	–	–	381	

[a] s: strong; w: weak; m: medium; sh: shoulder; v: very. [b] Intensities are approximate because are not specified. [c] Frequencies are approximate because are not specified. [d] Librational modes.

maining two IR bands around 910 and 415 cm^{-1} appear from the Al–OH librational modes.

The muscovite Raman dispersive (532 nm) and FT Raman spectra (1064 nm excitation line) are presented in Fig. 2. The obtained results are in good agreement with the literature data[7–9] (Table 3). Although the FT Raman spectrum (Fig. 2d) express higher noise-to-signal ratio, it is similar to its dispersive counterpart (Fig. 2c).

The higher frequency broad and complex band (around 1100 cm^{-1}) and the band around 900 cm^{-1} are assigned as stretching Si–O–Si(Al) vibrations (Table 3). Going towards lower wavenumbers, the very weak band around 750 and 700 cm^{-1} probably arises from the δ(O–Al–O) vibrations. The band at 541 cm^{-1} registered only in the FT Raman spectrum of muscovite from Dunje (Fig. 2 d), according to McKeown et al.[8] has Al–O–Al

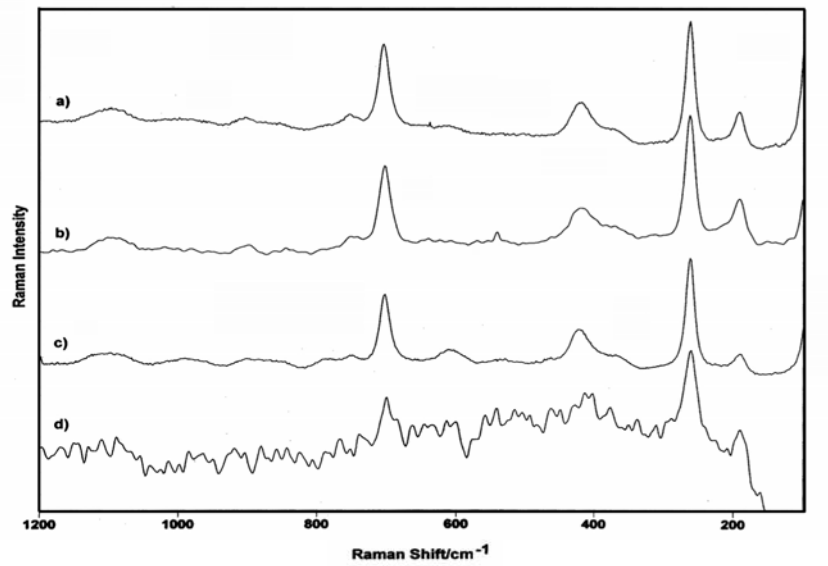

Fig. 2. Raman spectra of muscovite from Dunje (a and b) and Nežilovo (c and d) obtained using 532 and 1064 nm excitation line, respectively.

Table 3. Assignment of the bands in the Raman spectra of muscovite

This work (Dunje)[a]	This work (Dunje)[b]	This work (Nežilovo)[a]	This work (Nežilovo)[a]	Wada & Kamitakahara[7]	McKeown et al.[8]	Wopenka et al.[9]	Tentative assignment
1097 vw, br[c]	1102 w	1097 w	–	–	1098 w[d]	–	ν(Si–O–Si)
900 vw	899 w	902 vw	902 vw	895 w[d,e]	912 w	914 w	ν(Si–O–Al)
752 vw	753 vw	751 vw	752 vw	755 vw	754 w	756 w	δ(O–Al–O)
703 s	701 s	701 s	698 m	705 s	704 s	706 s	δ(O–Al–O)
–	541 w	–	–	–	542 w	566 w	δ(Al–O–Al)
419 m, br	420 m, br	420 m	420 w	425 s	410 s	417 s	δ(O–Al–O)
262 vs	262 vs	262 s	262 s	270 vs	265 vs	263 vs	δ(O–Si–O)
191 m	191 m	188 w	188 w	200 m	199 m	195 m	L(Al–OH)

[a] Excitation with the 532 nm line. [b] Excitation with the 1064 nm line. [c] s: strong; w: weak; m: medium; v: very; sh: shoulder; br: broad. [d] Intensities are approximate because they are not specified. [e] Frequencies are approximate because they are not specified.

bending character. The lower frequency bands around 420 and 260 cm^{-1} could not be solely prescribed to one vibrational type and have mixed character mainly associated to O–Al–O and O–Si–O translations. The Raman peak at 190 cm^{-1} could be attributed to Al–OH translations.

4. 2. Phlogopite, $KMg_3(Si_3Al)O_{10}(F,OH)_2$

The infrared spectrum of phlogopite in the 4000–400 cm^{-1} region is presented in Fig. 3a and band assignment is given in Table 4. The observed very weak intensity of the ν(OH) band at 3705 cm^{-1} (Fig. 3a, b) compared to the corresponding band in muscovite IR spectrum (Fig. 1a) is probably due to the difference in the molar OH absorption coefficients (~factor 3) between both minerals. Furthermore, a medium band registered at 1456 cm^{-1} (Fig. 3a) is neither expected nor observed in the corresponding literature data[4–6,13,14,16,32] (Table 4). It is explained by the presence of carbonate impurities in the sample supported by the fact that the band wavenumber strongly coincide with the corresponding one in the dolomite IR spectrum[33] shown in Fig. 3e. After treatment of the phlogopite sample by 3M HCl, the carbonate phase was totally removed (Fig. 3b).

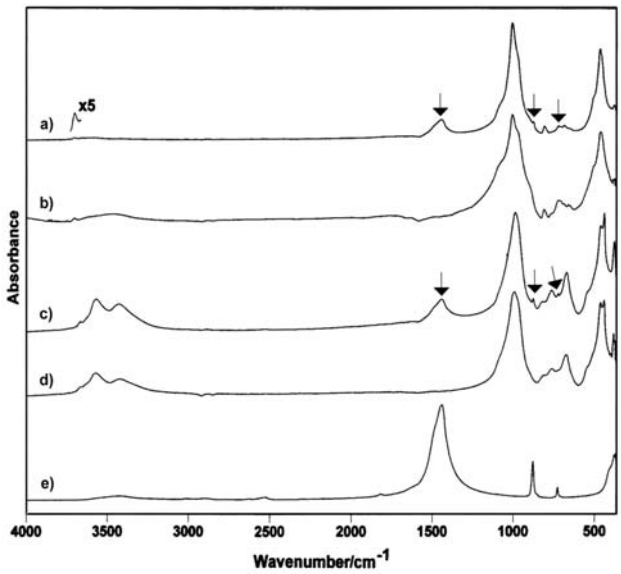

Fig. 3. FT IR spectra of phlogopite (a) and sheridanite (c) obtained using KBr pellets. The IR spectra of the samples after elimination of carbonate impurities (treatment by diluted HCl) are given under (b) and (d), respectively. IR bands that appear from dolomite (e) impurity are marked with arrows.

The Si–O–Si stretching spectral region of phlogopite is characterized by two bands (1011 and 977 cm^{-1}, Fig. 3a). In fact, the observed absorption at 977 cm^{-1} represents a shoulder (overlaped with the band at higher frequency) whereas in the literature,[4–6,12,13] a strong band has been reported (Table 4).

The weak bands found in the lower-frequency region (at 882, 813, 727 and 692 cm^{-1}) are also observed (except for the first one) by other authors[4–6,13,14,16] (Table 4). The 882 cm^{-1} band appears from the $\nu_2(CO_3^{2-})$ mode from the previously mentioned carbonate impurities (Fig. 3a), whereas the band at 813 cm^{-1} is probably associated with Al–O vibrations of AlO_4 tetrahedra[32]. On the other hand, the band at 727 cm^{-1} (overlapped with the $\nu_4(CO_3^{2-})$ mode from the carbonate impurities) arises from the Al–O–Si stretching vibrations[32] (Fig. 3c). The overlapping is additionally confirmed by sample treating with diluted HC-l solution (Fig. 3b). Namely, despite the complete elimination of the bands originating from the carbonate phase (Fig. 3a vs. Fig. 3b), the absorbance near 730 cm^{-1} remained (Fig. 3b). The band at 692 cm^{-1} is attributed to the symmetric Si–O–Si stretching vibration[4]. The absence of bands near 600 cm^{-1} from the OH librations (Fig. 3a) according to Farmer[32] is typical for fluorophlogopite although it might serve as an indication for phlogopite low OH molar absorption coefficient. The shoulder at 511 cm^{-1} and the band with very strong intensity at 470 cm^{-1} (Table 4) are assigned as the bending Si–O–Si modes[4–6,13,14,16].

The Raman spectrum of phlogopite sample was successfully recorded using the 514, 532 and 1064 nm excitation lines (Fig. 4, a, b and c). The peaks in the studied region (1200–100 cm^{-1}) are found at almost identical frequencies in all three spectra (Table 5). The highest-wave-

number doublet (around 1100 and 1085 cm^{-1}) appears from the strongest $\nu_1(CO_3^{2-})$ mode of the carbonate impurities: calcite (1086 cm^{-1}) and dolomite (1095 cm^{-1}) (Fig. 4, e and f). It is evident that, compared to the broader IR bands, the narrow Raman bands makes possible to clearly discriminate between the calcite and dolomite carbonate impurities in the studied phlogopite sample. In this context, Raman spectroscopy enables to differentiate between the isomorphous minerals. The band at 1032 cm^{-1} (also observed by McKeown et al.[15] and Wopenka et al.[9]) is attributed to the stretching Si–O–Si vibrations. The most prominent feature in the 700–300 cm^{-1} region is the strong band around 680 cm^{-1}. The broadening of its lower frequency side (as compared with the corresponding band in the muscovite spectrum), could be taken as an evidence for a greater tetrahedral Si/Al disorder in the phlogopite structure. This band probably arises from the tetrahedral O–Si(Al)–O bending vibration (the tetrahedral sites are 75% occupied by Si while the remaining 25% contain Al)[15]. The other weak bands found around 460, 370 and 320 cm^{-1} can not be unequivocally assigned because the bands originating from M–O translations (the octahedral sites occupied by Mg cations) are mixed with the tetrahedron deformation motions[15]. The exception are the peaks around 300, 280 and 170 cm^{-1} which obviously arise from carbonate (calcite and dolomite) impurities (see Fig. 4, e and f). The remaining bands at 116 and 104 cm^{-1} are tentatively attributed to K–O vibrations (Table 5).

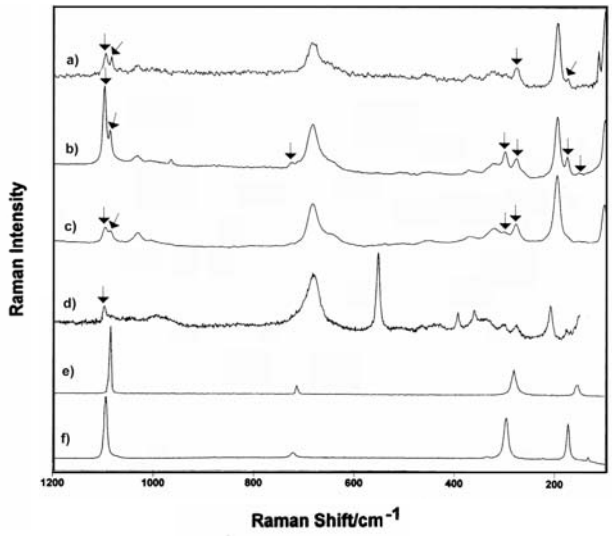

Fig. 4. Raman spectra of phlogopite (a, b, c) obtained using 514, 532 and 1064 nm excitation line, respectively, and sheridanite using 514 nm line (d). The Raman bands that appear from the calcite (e) and dolomite (f) impurities are marked with an arrows.

Table 4. Assignment of the bands in the powder infrared spectrum of phlogopite

This work	Stubičan & Roy[4]	Vedder[13]	Farmer & Russell[14]	Zeller & Juszli[5]	FDM spectra Canada[6]	Jenkins[16]	Tentative assignment
3705 vw[a]	3650 m[b, c]	3625 w	3704 w[b, c]	3700 w[b, c]	3701 w[b]	–	ν(OH)
1011 vs	1005 vs	1000 vs	–	1005 vs	1003 vs	995 vs	ν(Si–O–Si)
977 sh, s	960 vs	963 vs	960 s	960 vs	966 vs	916 vs	ν(Si–O–Si)
813 w	825 m	804 w	820 m	825 m	814 m	822 s	ν(Al–O–Al)
727 sh	730 w	728 w	730 sh	735 vw	744 m	725 w	ν(Al–O–Si) + carbonate imp.
692 m	690 m	708 w	690 w	690 m	682 m	690 s	ν_s(Si–O–Si)
511 sh	495 sh	497 sh	–	510 sh	522 s	520 vs	δ(Si–O–Si)
470 vs	465 vs	464 vs	–	465 vs	–	460 vs	δ(Si–O–Si)

[a] s: strong; w: weak; m: medium; v: very; sh: shoulder. [b] Intensities are approximate because are not specified. [c] Frequencies are approximate because are not specified.

Table 5. Assignment of the bands in the powder Raman spectra of phlogopite

This work[a]	This work[b]	This work[c]	Wopenka et al.[9]	McKeown et al.[15]	Tentative assignment
1032 w[d]	1032 w	1032 m	1030 w[e]	1034 w[e]	ν(Si–O–Si)
686 s	684 s	683 s	678 s	684 vs	δ(O–Si(Al)–O)
460 vw	464 vw	452 w	441 w	–	T(Mg–O)[f]
372 vw	373 w	374 w	–	373 w	T(Mg–O)
323 w	323 w	322 w	340 w	326 m	T(Mg–O)
280 m	279 m	279 m	282 w	282 m	T(MgO–H) + calcite imp.
197 vs	197 vs	197 vs	194 vs	199 vs	T(O–H)
116 m	–	–	–	–	T(K–O)
104 vs	103 vs	103 vs	–	–	T(K–O)

[a] Excitation with the 514 nm line. [b] Excitation with the 532 nm line [c] Excitation with the 1064 nm line. [d] s: strong; w: weak; m: medium; v: very; sh: shoulder. [e] Intensities are approximate because they are not specified. [f] Translation modes.

4. 3. Biotite, $K(Mg,Fe^{2+})_3AlSiO_{10}(OH,F)_2$

The infrared spectra of two collected biotite samples are presented in Fig. 5, a and b. Here, it should be pointed out that the sample found in Čanište locality was initially designated as vermiculite [$(Mg,Fe^{2+},Al)_3(Al,Si)_4O_{10}(OH)_2 \cdot 4H_2O$] because of the marked morphological similarities with this mineral. The obtained result from the chemical analysis are found to be very close and served as preliminary indication that samples belong to biotite: w.t. K_2O – 8.99%; Na_2O <0.01%; MgO – 10.49%; CaO <0.01%; FeO – 19.89%; SiO_2 – 36.23%; TiO_2 – 1.35%; MnO – 0.11%; Al_2O_3 – 13.45% (Čanište sample) and w.t. K_2O – 9.95%; Na_2O <0.01%; MgO – 10.04%; CaO <0.01%; FeO – 19.51%; SiO_2 – 36.79%; TiO_2 – 1.18%; MnO – 0.26%; Al_2O_3 – 15.09% (Pelagon sample). Moreover, the obtained IR spectrum using Nujol suspension mull (Fig. 5c) clearly demonstrates the presence of very weak bands from the surface adsorbed water around 3400 cm^{-1} (also registered in the IR spectra recorded using KBr pellets. The band assignments and the comparison with the literature IR data are listed in Table 6.

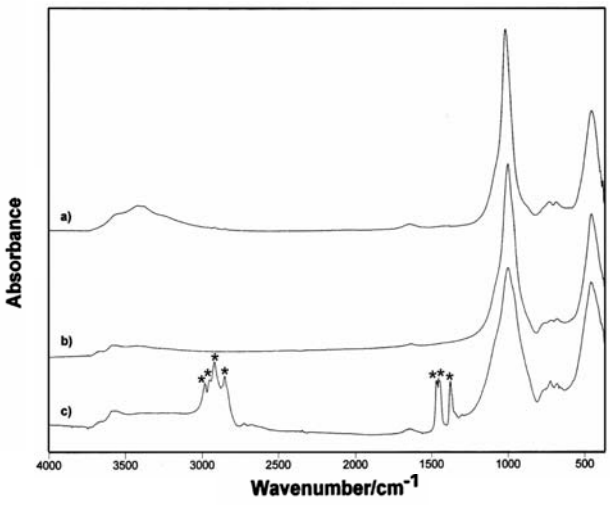

Fig. 5. FT IR spectra of biotite from Čanište (a) and Pelagon (b) obtained using KBr pellets. The FT IR spectrum of biotite from Čanište (c) recorded in Nujol mulls. The Nujol bands are denoted by asterisks.

The bands registered at 3556 cm^{-1} in the spectrum of the sample from Čanište and two bands in the spectrum of the sample from Pelagon (3675, 3555 cm^{-1}) are evidence for the presence of OH groups (Table 6).

The most intense maximum in the spectra of biotite is observed around 1010 cm^{-1} being in a very good agreement with the corresponding literature band[5,6] (Table 6). Although it has not been previously assigned, its appearance could be undoubtedly related to the ν(Si–O–Si) vibrations. In general, the bands around 720, 680 and 460 cm^{-1} are observed at frequencies close to those found in the literature[5,6]. Due to the lack of band assignments in the literature, the interpretation of the biotite (Table 6) spectra was based on the discussion concerning the previously studied sheet silicate minerals.

The identification of both biotite samples continued by the study of their Raman spectra obtained with 532 nm excitation line (Fig. 6) since the spectra obtained with 514.5 and 1064 nm excitation line were of very poor quality. Here, it should be pointed out that the Raman spectrum of biotite was compared with the corresponding very low quality spectra found in Internet databases[17,18] (not found in the literature). The assignment of the Raman bands was undertaken in the line with the discussion for the Raman spectra of the mica minerals. The highest-frequency peak around 1100 cm^{-1} present in both biotite spectra as well as in the Internet spectrum[17], appears as a result of ν(Si–O–Si) mode. The most intense bands in the 700–550 cm^{-1} spectral region are attributed to the Si–O–Si bendings, whereas the bands originating from the translational M–O (M = Mg, Fe) modes probably give rise to the maxima between 360 and 150 cm^{-1} (Table 7). The remaining peaks most likely arise from K–O translations.

It should be mentioned here that the IR spectra of phlogopite and biotite are very similar to each other. Exception is the appearance of the weak band at 813 cm^{-1} in the spectrum of phlogopite which is absent in the biotite spectrum.

Table 6. Assignment of the bands in the powder infrared spectra of biotite

This work (Čanište)	This work (Pelagon)	Zeller & Juszli[5]	FDM spectra Canada[6]	FDM spectra, Ontario[6]	Tentative assignment
–	3675 w[a]	–	3705 w[b]	3684 vw[b]	ν(OH)
3556 m	3555 m	3650 w[b, c]	–	–	ν(OH)
3427 m	–	3420 w	3429 w	3430 w	$\nu(H_2O)$ (adsorbed water)
3374 m	–	–	–	–	$\nu(H_2O)$ (adsorbed water)
1639 w	–	1625 w	1624 w	1629 w	$\delta(H_2O)$ (adsorbed water)
1015 vs	1002 vs	1010 vs	1001 vs	1005 vs	ν(Si–O–Si)
727 m	718 w	725 w	721 sh	725 w	ν(Al–O–Si)
682 m	681 m	680 w	688 w	682 w	ν(Si–O–Si)
455 vs	457 vs	460 vs	–	–	δ(Si–O–Si)

[a] s: strong; w: weak; m: medium; v: very; sh: shoulder. [b] Frequencies are approximate because are not specified. [c] Intensities are approximate because are not specified.

Table 7. Assignment of the bands in the powder Raman spectra of biotite

This work (Pelagon)[a]	This work (Čanište)[a]	Ref.[17]	Ref.[18]	Tentative assignment
1093 w[b]	1096 w	1100 w[c,d]	–	ν(Si–O–Si)
–	–	760 m	–	
673 s	669 m	670 m	690[c]	δ(Si–O–Si)
587 s	588 s	560 s	–	δ(Si–O–Si)
354 m	371 w	370 m	–	T(M–O)[e, f]
309 m	–	–	310	T(M–O)
–	292 w	270 w	275	T(M–O)
183 vs	189 s	–	190	T(M–O)
148 w	140 w	–	–	T(K–O)
–	106 w	–	104	T(K–O)

[a] Excitation with the 532 nm line. [b] s: strong; w: weak; m: medium; v: very. [c] Frequencies are approximate because they are not specified. [d] Intensities are approximate because they are not specified. [e] Translational modes. [f] M = Mg or Fe.

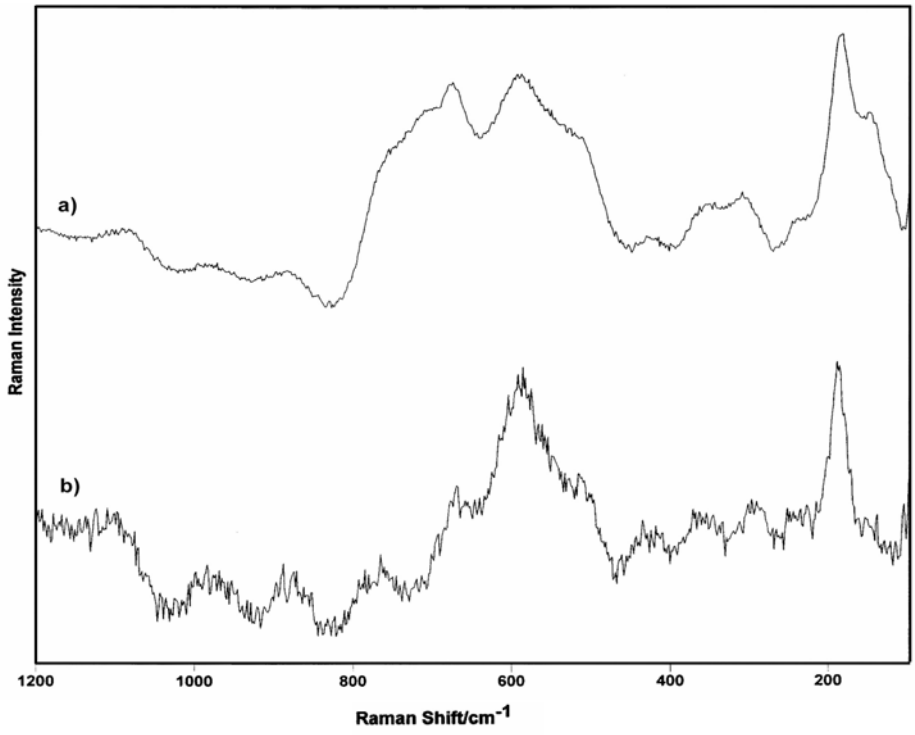

Fig. 6. Raman spectra of biotite from Pelagon (a) and Čanište (b) obtained using 532 nm excitation line.

4. 4. Sheridanite, $(Mg,Al)_6(Si,Al)_4O_{10}(OH)_8$

Similarly to the wrong preliminary contemplation of biotite as vermiculite, this mineral sample was initially morphologically characterized as kossmatite, Ca_3Mg-$Al_2AlSi_3O_{10}(OH,F)_9$. However, the results of the X-ray microprobe analysis of the sample from Sivec (CaO – 0.25%; MgO – 34.58%; SiO_2 – 28.38%; TiO_2 – 0.02%; Al_2O_3 – 23.31%; Na_2O – 0.51%; K_2O – 0.04%) compared to the chemical composition of kossmatite published by Erdmannsdöffer[34] (SiO_2 – 28.47%; $A1_2O_3$ – 22.84%; Fe_2O_3 – 0.26%; MgO – 8.16%; CaO – 27.10%; Na_2O – 0.51%; K_2O – 0.07%; F – 1.14%; H_2O^+ – 11.69%; H_2O^- – 0.82%) showed that our studied specimen is not kossmatite. The finding is in the line with the result of the Barić[35] who mentioned that kossmatite mineral (found in the dolomite marble from Sivec, Macedonia) was not a new mineral specie and most likely was mistaken with margarite. Furthermore, the obtained data for the chemical composition of the studied sample are very close to those found for chlorite[35] (SiO_2 – 28.21%; Al_2O_3 – 24.64%; FeO – 0.16%; MgO – 33.13%; Na_2O – 0.14%; K_2O – 0.19%; H_2O^+ – 12.97%; H_2O^- – 0.82%). According to Strunz classification system[26] several mineral species belong to the chlori-

te group and the studied sample, based on the before mentioned chemical analysis, is recognized as the sheridanite variety of Mg-rich chlorite (clinochlore). Its infrared spectrum is presented in Fig. 3c, whereas the band assignments (Table 8) were based on the previously studied IR spectrum of clinochlore[1] (IR data for sheridanite are not found in the literature).

The IR spectrum (4000–400 cm^{-1}) is characterized by well-defined sharp bands, probably due to the high degree of structural order in this mineral. The appearance of three bands (at 3670, 3567 and 3431 cm^{-1}) from the ν(OH) stretching vibrations (Fig. 3c) is in agreement with the presence of three crystallographically different OH groups in the clinochlore structure. According to Prieto et al.[36] the first one (at 3670 cm^{-1}) originates from OH groups not involved in hydrogen bonding, whereas the remaining two (at 3567 and 3431 cm^{-1}) arise from OH groups participating in the formation of hydrogen bonds. The band with medium intensity observed at 1449 cm^{-1} (Fig. 3, c and e) undoubtedly originates from the presence of the carbonate impurities since the chlorites in Sivec are associated with marbles[33]. The carbonate phase is also associated to the bands at 881 and 728 cm^{-1} due to the $\nu_2(CO_3^{2-})$ and $\nu_4(CO_3^{2-})$ mode, respectively. After treatment of the sample in 3 M HCl, the carbonate phase was totally eliminated (Fig. 3d).

The most characteristic band in the IR spectrum of sheridanite (found at 993 cm^{-1}) arises from Si–O–Si stretching vibrations (Table 8). The bands found at 820 and 765 cm^{-1} most likely appear as a result of ν(Al–O) vibrations, whereas the band at 677 cm^{-1} could be attributed to either symmetric Si–O–Si stretching mode or metal-hydroxyl libration. The bending Si–O–Si modes give rise to the strong band at 444 cm^{-1} accompanied by the shoulder at 543 cm^{-1}. The remaining strong bands observed at 465 and 382 cm^{-1} originate from the Mg–OH libration and carbonate contamination, respectively.

Table 8. Assignment of the bands in the powder infrared and Raman spectrum of sheridanite

Infrared		Raman	
This work	**Tentative assignment**	**This work[b]**	**Tentative assignment**
3670 vw[a]	ν(OH)	994 w	ν_{as}(Si–O–Si)
3567 m	ν(OH)	683 vs	ν_s(Si–O–Si)
3431 m	ν(OH)	553 vs	δ(Si–O–Si)
993 vs	ν(Si–O–Si)	436 w	δ(Si–O–Si)
820 vw	ν(Al–O)	393 m	δ(Si–O–Si)
765 m	ν(Al–O)	361 m	δ(Si–O–Si)
677 m	ν_s(Si–O–Si) or L(Mg–OH)[c]	276 w	T(M–O)[d]
543 sh	δ(Si–O–Si)	209 m	T(M–O)
465 vs	L(Mg–OH)		
444 s	δ(Si–O–Si)		

[a] s: strong; w: weak; m: medium; v: very; sh: shoulder. [b] Excitation with the 514 nm line. [c] Librational modes. [d] Translational modes.

The Raman spectrum of sheridanite recorded with the 514 nm excitation line is shown in Fig. 4d. Similarly to the IR spectrum, the Raman data for sheridanite have not been reported in the literature. The highest-frequency peaks found at 1098 and 994 cm^{-1} are attributed to the $\nu_1(CO_3)$ mode from the carbonate impurities (Fig. 4, f) and to the antisymmetric Si–O–Si stretching modes, respectively (Table 8). The symmetric Si–O–Si stretching mode is represented by the very strong peak at 683 cm^{-1}, whereas the δ(Si–O–Si) mode gives rise to the maxima at 553, 436, 393, 361 cm^{-1} (Fig. 4d). Four peaks are noticed in the 300–150 cm^{-1} spectral region (at 300, 276, 209 and 176 cm^{-1}) and except for the first and the fourth ones (carbonate impurities) (Fig. 4, f), the remaining could be assigned to metal–oxygen translations (Table 8).

5. Conclusions

It was shown that, in general, vibrational spectroscopy gives preliminary, but very significant, information about several geologically important phyllosilicate minerals. Here, it should be pointed out that, in the case of mica minerals which are characterized with many chemical substitution and complicated crystal structure, vibrational spectroscopy can not enable quick and simple discriminations. Additional difficulties might introduce the presence of impurities in the mineral samples.

In the case of mica minerals the identification should not be based solely on the morphological features of the minerals and on vibrational spectroscopy that could sometimes led to wrong identification. Such was the case with the samples of muscovite (Nežilovo) being initially designated as paragonite. In this context, the results from the XRD and chemical analysis should be additionally taken into account for their proper characterization.

Some difficulties that appear in the identification process arise mainly from the presence of impurities in the mineral samples. Thereby it could be concluded that here Raman spectrsocopy was found to be more powerful technique since it enables to differentiate between the isomorphous calcite and dolomite impurities. The broader bands in the IR spectra could not be used to distinguish between the mentioned impurities of the isomorphous carbonates.

6. Acknowledgements

We cordially thank the anonymous reviewers for the constructive comments and suggestions. The financial support from the Ministry of Education and Science of the Republic of Macedonia is gratefully acknowledged. The authors sincerely thank Dr. Andreja Gajović from the Rudger Bošković Institute, Zagreb and Dr. Tomislav Biljan from the Faculty of Science, Zagreb, Croatia for re-

cording the Raman spectra with 514.5 and 1064 nm, respectively.

7. References

1. V. Šontevska, G. Jovanovski, P. Makreski, *J. Mol. Struct.* **2007**, *834–836*, 318–327.
2. D. G. Taylor, C. M. Nenadic, J. V. Crable, *Amer. Ind. Hyg. Ass. J*. **1970**, *31*, 100–108.
3. W. Vedder, R. S. McDonald, *J. Chem. Phys*. **1963**, *38* 1583–1590.
4. V. Stubičan, R. Roy, *Am. Mineral*. **1961**, *46*, 32–51.
5. M. V. Zeller, M. P. Juszli: Infrarot-Vergleichsspektren von Mineralien, Angewandte Infrarotspektroskopie, Heft 16, Bodenseewerk Perkin-Elmer & Co GmbH, Überlingen, **1975**.
6. http://www.fdmspectra.com/.
7. N. Wada, W. A. Kamitakahara, *Phys. Rev. B* **1991**. *43* 2391–2397.
8. D. A. McKeown, M. I. Bell, E.S. Etz, *Am. Mineral*. **1999**, *84*, 1041–1048.
9. B. Wopenka, R. Popelka, J. D. Pasteris, S. Rotroff, *Appl. Spectrosc*. **2002**, *56*, 1320–1328.
10. K. Langer, N. D. Chatterjee, K. Abraham, *N. Jb. Min. Abh.* **1981**, *142*, 91–110.
11. A. Beran, *Rev. Mineral. Geochem*. **2002**, *46*, 351–369.
12. A. Papin, J. Sergent, J. L. Robert, *Eur. J. Mineral.* **1997**, *9*, 501–508.
13. W. Vedder, *Am. Mineral*. **1964**, *49*, 736–768.
14. V. C. Farmer, J. D. Russell, *Spectrochim. Acta* **1964**, *20*, 1149–1173.
15. D. A. McKeown, M. I. Bell, E. S. Etz, *Am. Mineral.* **1999**, *84*, 970–976.
16. D. M. Jenkins, *Phys. Chem. Min.* **1989**, *16*, 408–414.
17. http://www.fis.unipr.it/phevix/ramandb.html
18. http://wwwobs.univ-bpclermont.fr/sfmc/ramandb2/index.html
19. G. Jovanovski, P. Makreski, B. Šoptrajanov, B. Kaitner, B. Boev, *Contributions, Sec. Math. Tech. Sci., MANU*, **2005**, *26*, 7–84.
20. W. D. Nesse: Introduction to Mineralogy, Oxford University Press, New York, **2000**.
21. D. Slovenec, V. Bermanec: Sistematska Mineralogija – Mineralogija Silikata, Denona d.o.o., Zagreb, **2003**.
22. N. Guven, *Z. Kristallogr.* **1971**, *134*, 196–212.
23. L. Cheng-Yi, S.W. Bailey, *Am. Mineral.* **1984**, *69*, 122–127
24. V. Busigny, P. Cartigny, P. Philippot, M. Javoy, *Am. Mineral*. **2004**, *89*, 1625–1630.
25. G. J. Redhammer, A. Beran, J. Schneider, G. Amthauer, W. Lottermoser, Am. Mineral. **2000**, *85*, 449–465.
26. H. Strunz, E.H. Nickel, Strunz Mineralogical Tables (Ninth Ed): Chemical Structural Mineral Classification System, Schweizerbart'sche Verlagsbuchhandlung, Germany, **2001**.
27. http://www.galleries.com/
28. R. Rothbauer, *Neues J. Miner. Monat*. **1971**, 143–154.
29. R. M. Hazen, C. W. Burnham, *Am. Mineral.* **1973,** *58* 889–900.
30. S. B. Hendricks, M. E. Jefferson, *Am. Mineral*. **1939**, *24*, 729–771.
31. R. C. McMurchy, *Z. Kristallogr*. **1934**, *88*, 423.
32. V. C. Farmer, in: V .C. Farmer (Ed.): The Infrared Spectra of Minerals, Mineralogical Society, London, **1974**, pp. 331–358.
33. G. Jovanovski, V. Stefov, B. Šoptrajanov, B. Boev, *N. Jb. Miner. Abh,* **2002**, *177*, 241–253.
34. O. H. Erdmannsdöffer, Cbl. Miner. Geol. Paläont. **1925**, Abt. A, 69–72.
35. Lj. Barić, *Tschermaks Miner. Petrogr. Mitt*. **1969**, *13*, 233–249.
36. A. C. Prieto, J. Dubessy, M. Cathelineau, *Clay. Clay Miner*. **1991**, *39*, 531–539.

Povzetek

Vibracijski (infrardeči in Ramanski) spektri plastovitih silikatnih mineralov: biotita, $K(Mg,Fe^{2+})_3AlSiO_{10}(OH,F)_2$; muskovita, $KAl_2(Si_3Al)O_{10}(OH,F)_2$; flogopita, $KMg_3(Si_3Al)O_{10}(F,OH)_2$ and šeridanita (klinoklora), $(Mg,Al)_6(Si,Al)_4O_{10}(OH)_8$, zbranih z različnih lokacij v republiki Makedoniji, so bili opisani in interpretirani. Omenjeni minerali izkazujejo IR spektralne podobnosti v območju pod 1200 cm^{-1}. V splošnem so bili trakovi v območju 1100–900 cm^{-1} asignirani kot ν(Si–O–Si), dočim večina nizko frekvenčnih trakov razložimo z ali δ(OH) ali δ(Si–O–Si) vibracijami. Avtentičnost vzorcev je bila preverjena z rentgenskimi metodami in kemijsko analizo.